An Experimental Electron Density Investigation of Squarate and Croconate Dianions

Anupama Ranganathan and G. U. Kulkarni*

Chemistry and Physics of Materials Unit, Jawaharlal Nehru Centre for Advanced Scientific Research, Jakkur, Bangalore 560 064, India

Received: October 19, 2001; In Final Form: June 10, 2002

A comparative study of the structure and topography of charge density in the squarate and croconate dianions has been carried out on the basis of low-temperature X-ray diffraction measurements. Both the dianion rings exhibit a high degree of planarity with uniform C−C bond lengths and angles. The bond critical points in the two dianions carry similar densities as well as Laplacians. Deformation density maps reveal that the squarate ring is more strained than the croconate. Both the rings exhibit (3, +1) ring critical points. The density and the Laplacian associated with the ring critical point of the squarate anion are 0.59 e $Å^{-3}$ and 11.8 e $Å^{-5}$, respectively, whereas for the larger croconate ring, they are nearly one-half these values. Ring critical point parameters of the dianions have been compared with those of several aromatic as well as nonaromatic cyclic systems.

Introduction

The electronic charge density method of X-ray crystallography is being increasingly employed to study diverse aspects of molecular systems.[1,2] For instance, the nature of the hydrogen bonds in proton sponges and the charge redistribution occurring upon protonation have been investigated using the electron density and its Laplacian by Mallinson et al.[3] The biomolecular functionality of amino acids and oligopeptides have been extensively studied by way of analyzing their electrostatic potentials.[4] In-crystal molecular properties related to nonlinear optical activity[5,6] and pyroelectricity[7] have been evaluated by employing experimental charge density. Recently, a quinoid-based complex with a wide charge separation between the donor and the acceptor groups has been investigated.[8]

Aromaticity of cyclic molecules[9] is an aspect barely explored by experimental charge density analysis although a number of aromatic systems have been investigated during the last two decades by this method. Cameron et al.[10] studied the topography of the electron density of benzene molecule trapped inside a phosphazene crystal and provided evidence for the π-density above and below the ring planes. The charge density of a neat benzene crystal was examined by Spackman et al.[11] who derived the quadrupolar moment. Electron delocalization in citrinin[12] and in an annulene derivative[13] has been analyzed in terms of the critical point parameters. There has been an effort to obtain information on the extent of conjugation in N-containing compounds such as imidazole,[14] triazole,[15] and pyrimidine derivatives,[14] based on the bond properties. Though the electron densities at the bond critical points were found to be intermediate to those of single and double bonds akin to aromatic rings, the Laplacian and the ellipticity values hardly showed any systematic trend. Koritsanszky and Coppens[1] point out that the bond properties obtained from the charge density alone may not provide a consistent description of aromaticity involving electron delocalization and should therefore be formulated in terms of the collective rather than the local parameters. Howard and Krygowski[16] in their theoretical study of benzenoid hydrocarbons, emphasize that the charge density descriptors evaluated at the ring critical point (RCP) are more suitable for describing the aromatic character of a molecule.

We considered it interesting to examine the charge density distributions in oxocarbon rings, which have formed a subject of great interest ever since West et al.[17] pointed out that these 2π electron ring dianions constitute a new aromatic system. West and Powell[18] calculated delocalization energies using the Hückel LCAO-MO method and predicted that the delocalization energy per π electron was substantial for all the oxocarbon dianion species but fell sharply with increasing ring size. The use of delocalization energy as a measure of aromaticity is, however, questionable.[19] On the basis of the graph theory of aromaticity, Aihara[20] concluded that the degree of aromaticity in the oxocarbon dianions decreases with increasing ring size, as found by other workers as well.[21] Schleyer et al.[22] have analyzed the degree of aromaticity in the oxocarbon dianions on the basis of magnetic properties and found the deltate anion to be doubly aromatic (both σ and π aromatic), the squarate moderately aromatic and the croconate to be relatively less aromatic. Very recently, Quiñonero et al.[23] used the nucleus independent chemical shifts (NICS), Wiberg bond indices, and ^{17}O NMR calculated chemical shifts while dealing with the aromaticity of the oxocarbon anions.

In this paper, we have carried out a comparative investigation of the squarate, $C_4O_4^{2-}$, and the croconate, $C_5O_5^{2-}$ anions by the experimental charge density method, the analysis of the croconate dianion being reported for the first time. For this purpose, we have carried out high-resolution X-ray diffraction measurements on single crystals at low temperatures. We have analyzed the topography of the charge distribution in both the anion ring regions. We have also compared the charge density parameters at the ring critical points (RCP) of these two dianions with those of other cyclic systems reported in the literature. Our study provides some insight into the conjugation in the two anion rings and also shows how one may classify aromatic and nonaromatic rings on the basis of the density and the Laplacian at RCP.

* For Correspondence. E-mail: kulkarni@jncasr.ac.in.

10.1021/jp013902a CCC: $22.00
Published on Web 08/06/2002

TABLE 1: Crystal Structure Data for Disodium Squarate Trihydrate and Disodium Croconate Trihydrate

chemical formula	$Na_2C_4O_4 \cdot 3H_2O$	$Na_2C_5O_5 \cdot 3H_2O$
formula weight	212.07	240.08
cell setting	triclinic	monoclinic
space group	$P\bar{1}$	$P2_1/c$
a (Å)	6.9879(10)	6.3444(10)
b (Å)	8.0949(10)	13.099(3)
c (Å)	8.2286(10)	10.662(3)
α (deg)	113.12	90
β (deg)	100.04	105.87(2)
γ (deg)	111.62	90
ρ (Mg/m^3)	1.907	1.871
μ, mm^{-1}	0.276	0.260
cell volume (Å^3)	369.24(8)	852.3(3)
crystal size (mm)	0.50 × 0.13 × 0.30	0.22 × 0.33 × 0.33
crystal color	colorless	yellow
Z	2	4
F(000)	216	488
diffractometer	Siemens CCD 3 circle diffractometer	Siemens CCD 3 circle diffractometer
radiation type	Mo Kα (0.71073 Å)	Mo Kα (0.71073 Å)
crystal−detector dist (cm)	5.0	5.0
temp (K)	130(2)	130(2)
no. of measd reflns	11165	12439
no. of ind reflns	6254	6915
no. of obsd reflns	4324	4144
R_{merge}[a]	0.0683	0.08
R_{int}[a]	0.0392	0.043
θ_{max} (deg), sin θ/λ (Å^{-1})	49.45, 1.07	49.17, 1.06
range of h, k, l	$-13 \le h \le 14$ $-17 \le k \le 17$ $-17 \le l \le 16$	$-12 \le h \le 12$ $-26 \le k \le 22$ $-21 \le l \le 13$
refinement		
refinement on F^2		
$R(F)$	0.0397	0.0483
$wR(F^2)$	0.1004	0.1134
S	0.960	0.940
no. of reflns used in the refinement	6254	6915
no. of params refined after multipole refinement	142	160
weighting scheme	0.0472, 0.094	0.057, 0.1138
$R\{F\}$	0.0366	0.0392
$R\{F^2\}$	0.07	0.064
S	1.0496	1.196
no. of variables	245	263
N_{ref}/N_v	25.8122	23.0342
Cambridge Crystallographic Database deposition no.	CCDC 171698	CCDC 171699

[a] $R_{merge} = \Sigma|F_o^2 - F_o^2(\text{mean})|/\ \Sigma[F_o^2]$. $R_{int} = \Sigma[\sigma(F_o^2)]/\Sigma[F_o^2]$.

Experimental and Refinement Section

The disodium salt of squaric acid was prepared by the addition of 10 mL of 1 M NaOH to a saturated solution of 0.114 g (1 mmol) of squaric acid (Aldrich) in water. Colorless crystals grown from the aqueous solution by slow evaporation at room temperature were separated and washed with water. The disodium salt of croconic acid was procured commercially (Aldrich) and yellow-colored crystals were obtained from a saturated solution of the compound in water, by slow evaporation at room temperature. High quality crystals of the two compounds were chosen after examination under an optical microscope. X-ray diffraction intensities were measured by ω scans using a Siemens three-circle diffractometer attached with a CCD area detector and a graphite monochromator for the Mo Kα radiation (50 kV, 40 mA). The crystals were cooled to 130 K on the diffractometer using a stream of cold nitrogen gas from a vertical nozzle and the temperature was maintained within 1 K throughout the data collection.

The unit cell parameters and the orientation matrix of the crystal were initially determined using ∼45 reflections from 25 frames collected over a small ω scan of 7.5° sliced at 0.3° interval. A full-sphere data set of the reciprocal space was collected in two shells for the squarate crystal (triclinic system) with 2θ settings of the detector at 28° and 70° in order to increase redundancy in the data. In the case of croconate (monoclinic system), a hemisphere of data of the reciprocal space with similar 2θ settings was collected. Data reduction was performed using the SAINT program (Siemens, 1995) and the orientation matrix along with the detector and the cell parameters were refined for every 40 frames on all the measured reflections. The experimental details for the two systems are listed in Table 1. Absorption correction was applied for both the systems using the SADABS program (Siemens, 1995). The crystal structures were first determined with the low-resolution data up to sin $\theta/\lambda = 0.56$ Å^{-1}. The phase problem was solved by direct methods and the non-hydrogen atoms were refined anisotropically, by means of the full-matrix least-squares procedure using the SHELXTL program (Siemens, 1995). All the hydrogens were located using the difference Fourier method. The triclinic form of disodium squarate trihydrate and the monoclinic form of disodium croconate trihydrate are being reported by us for the first time (CCDC numbers 171698 and 171699, respectively). In addition, a triclinic form of the croconate was also obtained, but the high-resolution data were not collected for this polymorph.

Charge density analysis was carried out on the basis of multipole expansion of the electron density centered at the nucleus of the atom. Accordingly, the aspherical atomic density

can be described in terms of spherical harmonics,

$$\rho_{atom}(r) = \rho_{core}(r) + \rho_{valence}(r) + \rho_{def}(r)$$

Thus for each atom,

$$\rho_{atom}(r) = \rho_{core}(r) + P_V\kappa^3\rho_{valence}(\kappa r) + \sum_{l=0}\kappa'^3 R_l(\kappa'\xi r)\sum_{m=0}\sum_{p=\pm l} P_{lmp}Y_{lmp}(\theta,\varphi)$$

with the origin at the atomic nucleus. The population coefficients, P_{lmp}, are to be refined along with the κ and κ' parameters, which control the radial dependence of the valence shell density. The analysis was carried out in several steps.

The H atom positions were found using the difference Fourier method and were adjusted to average neutron values[24] as commonly done during the multipole refinement (O−H, 0.96 Å). A high-order refinement of the data was performed using reflections with sin $\theta/\lambda \geq 0.6$ Å^{-1} and $F_o \geq 4\sigma$. All the hydrogens were held constant throughout the refinement along with their isotropic temperature factors. Multipolar refinement for the charge density analysis was carried out using the XDLSM routine of the XD package,[25] and the details are given in Table 1. The atomic coordinates and the thermal parameters obtained from the high-order refinement were used as input to XD refinement. Sodium atoms were refined up to hexadecapole moments and carbon and oxygen up to octopole, but hydrogens were restricted to dipole. Chemical constraint was applied on the sodium ions and carbon and oxygen atoms of the anion rings.[26] The charge neutrality constraint was applied to the asymmetric unit in both the cases. κ refinement was carried out on both the spherical and deformation valence shells of the non-hydrogen atoms, whereas those for the hydrogens were restricted to the spherical valence. The multipolar refinement strategy was the following: (a) scale factor, (b) P_V, (c) P_{lm} (steps b and c until convergence), (d) κ, (e) steps b and c until convergence, (f) κ', (g) steps b and c until convergence, (h) positional and thermal parameters of all the non-hydrogen atoms, and finally, (i) P_V and P_{lm} together. Difference mean square displacement amplitudes (DMSDA) for the various bonds obtained from XD were found to follow closely the Hirshfeld criterion.[27]

The XDPROP routine was used to calculate the total electron density, $\rho(r)$, the Laplacian, $\nabla^2\rho$ and the ellipticity, ϵ, at the bond critical points (BCPs) as well as ρ and $\nabla^2\rho$ at the ring critical points (RCPs). The static deformation density (total density − promolecular density) maps have been plotted using the XDGRAPH routine. The residual maps in different planes of the molecule were featureless.

Results and Discussion

The asymmetric units of the two compounds, disodium squarate trihydrate and disodium croconate trihydrate with atom labeling are shown in Figure 1 and the crystal data and other experimental details are listed in Table 1. The asymmetric unit in both the cases consists of an anion ring, two sodium cations, and three water molecules. The structure of the squarate salt reported here belongs to a triclinic, $P\bar{1}$ space group, as distinct from the reported monoclinic form.[28] In both the forms, the anions are arranged in stacks, the spacing being 3.48 Å in the monoclinic form as compared to 3.37 Å in the triclinic form (both being close to the 3.40 Å separation expected for aromatic systems). The major difference between the two forms is in the octahedral coordination around the sodium ion. In the triclinic form reported here, four oxygens from water molecules and two from the squarate rings form the coordination shell, whereas in the monoclinic form, water molecules and the squarate rings contribute an equal number of oxygens to the coordination.

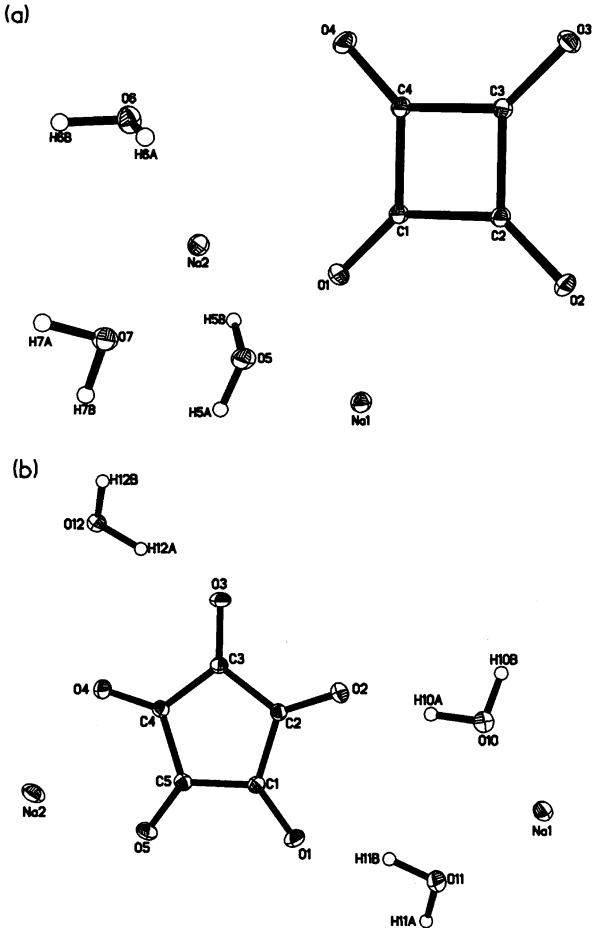

Figure 1. Asymmetric units of (a) disodium squarate trihydrate and (b) disodium croconate trihydrate. Thermal ellipsoids are shown at 50% probability.

The croconate salt (Figure 1b), occurs in a monoclinic $P2_1/c$ space group. Its structure is quite similar to that of potassium croconate dihydrate reported by Dunitz et al.[29] The interplanar spacing in the potassium salt is about 3.30 Å as compared to 3.20 Å in the present case. The potassium ion is surrounded by oxygen atoms of four separate anions and to the oxygen atom of a water molecule, which is somewhat different compared to the coordination of the sodium ion. In the sodium croconate trihydrate, the sodium ion is surrounded by three oxygen atoms from water molecules and a carbonyl oxygen from the neighboring croconate ring.

The C−C distances in each ring are quite similar, the mean values being 1.471(9) and 1.468(2) Å for the squarate and the croconate rings, respectively. Likewise, the C−O bonds of the anions are nearly equal with mean values of 1.259(6) and 1.248(4) Å. The corresponding C−C−C angles are 90° and 108° within 0.5°, but the O−C−C angles exhibit a larger spread especially for the croconate ion. Both the squarate and the croconate rings are essentially planar, the mean deviation of the atoms being ∼0.007 and ∼0.009 Å, respectively.

The oxocarbon dianions in both the salts are actively involved in hydrogen bonding with the surrounding water molecules (Figure 2). Atom O(2) of the squarate ring forms trifurcated O−H···O bonds with water molecules at H···O distances of 1.714(13), 1.873(12), and 1.938(10) Å, whereas O(4) forms a bifurcated bond with two water molecules, the H(5A)···O(4)

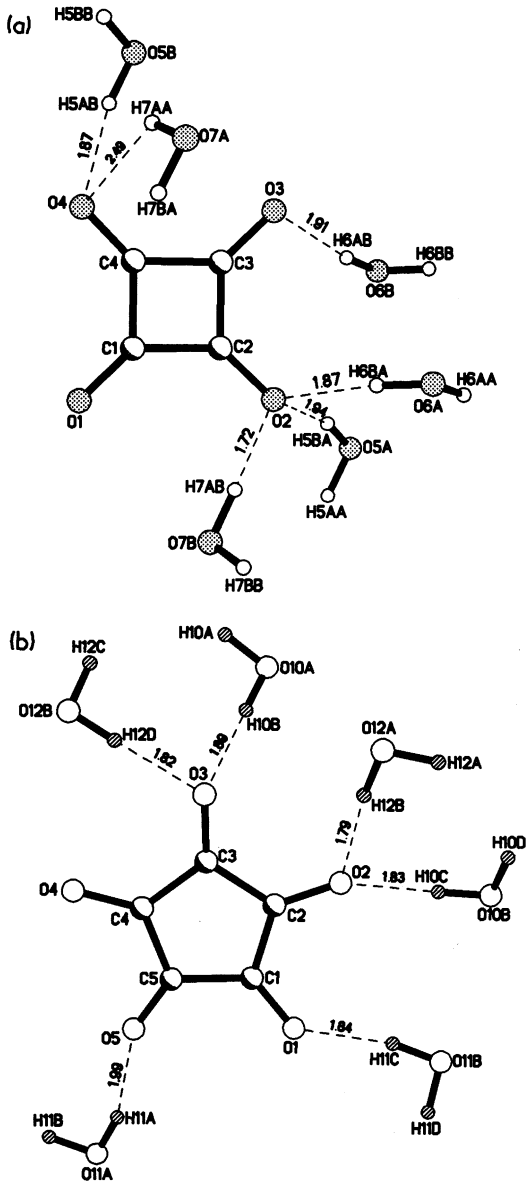

Figure 2. Hydrogen bonding patterns in (a) disodium squarate trihydrate and (b) disodium croconate trihydrate. The hydrogen bond distances are indicated.

bond (1.871(19) Å, 163.8(19)°) being stronger than the H(7A)···O(4) bond (2.497(17) Å, 131.0(13)°). Besides, there exists a linear O−H···O bond between H(6A) and O(3) at 1.912(8) Å, 166.4(12)°. In the disodium salt of croconic acid, O(2) and O(3) of the dianion form bifurcated hydrogen bonds with the water molecules at distances spread between 1.80 and 1.89 Å and angles between 171° and 176°. Linear O−H···O bonds exist between O(1) and H(11B) (1.841(5) Å, 166.9(17)°) as well as between O(5) and H(11A) (1.998(7) Å, 164.5(15)°). Besides hydrogen bonding interactions, ionic interactions between the ring oxygen atoms and the sodium cations are observed in both the salts at distances of ∼2.5 Å.

In Figure 3, the static deformation densities in the ring planes are shown. Concentric contours typify the various bonding regions in the molecule between the atom cores. In the squarate ring, the C−C bonding density appears spread out of the square frame, implying that the ring is considerably strained (Figure 3a). On the other hand, the C−C bonding density in the croconate ring (Figure 3b) appears more uniform across the internuclear axes. The bonding density in the C−O bond regions is more toward the electropositive carbon atom. The lone pair

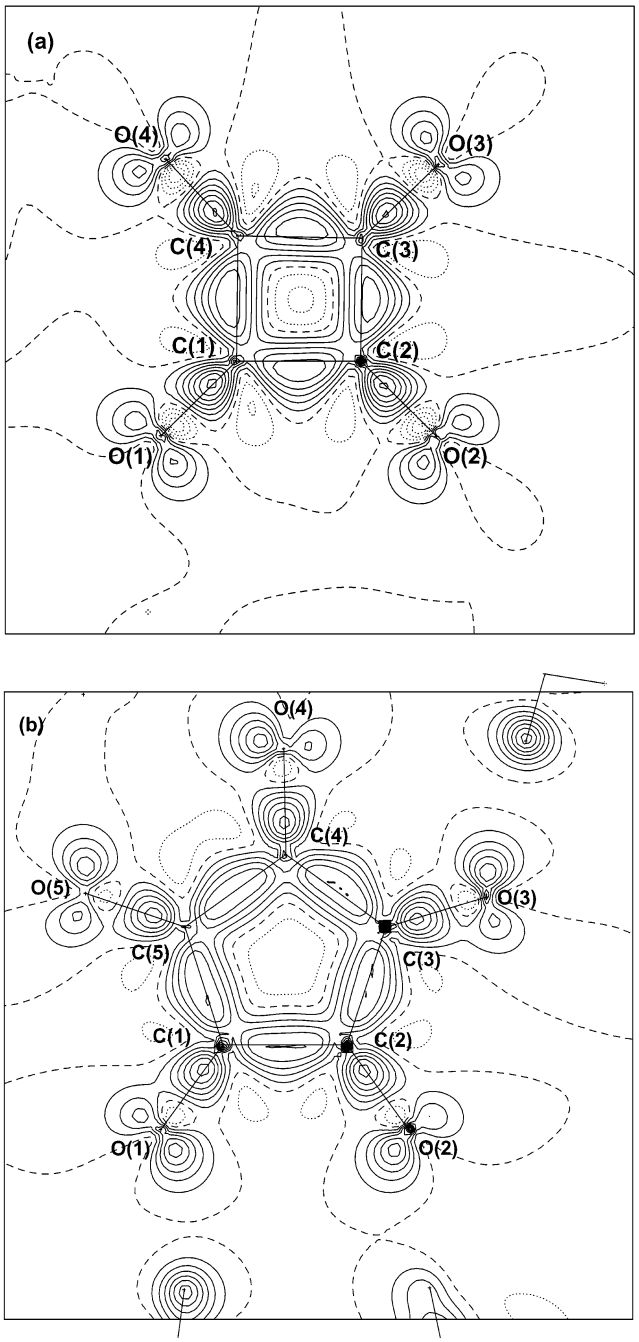

Figure 3. Deformation density maps in the dianion ring plane for (a) the squarate and (b) the croconate. Contour interval at 0.1 e Å^{-3}.

lobes on the oxygens are also clearly seen in the figure. The map of the squarate ring is similar to the one reported by Lee et al.,[30] who examined crystals of tetraaqua transition metal squarate complexes.

The topography of the charge density in the bonding regions is usually quantified by the critical point (CP) analysis.[31] The set (rank, signature) associated with a critical point describes its nature. For all stable molecules, the rank, which is the number of nonzero eigenvalues of the Hessian matrix of the electron density, is 3. The signature, which is the sum of the three eigenvalue sign factors, takes values of −3 (local maximum), −1 (first-order saddle), +1 (second-order saddle), and +3 (local minimum) associated with nucleus, bond, ring, and cage, respectively. In a given bond, the location of the critical point with respect to the bonding atoms and the values of the various parameters at that point signify properties of the bond under

TABLE 2: Bond Critical Points in the Oxocarbon Dianions[a]

bond	ρ (eÅ^{-3})	$\nabla^2\rho$ (eÅ^{-5})	ϵ
	(a) Squarate		
C(1)−C(2)	1.87(1)	−13.38(2)	0.25
C(2)−C(3)	1.87(1)	−13.57(1)	0.27
C(3)−C(4)	1.87(1)	−13.54(1)	0.25
C(4)−C(1)	1.85(1)	−12.96(2)	0.23
O(1)−C(1)	2.73(2)	−32.75(8)	0.19
O(2)−C(2)	2.68(1)	−30.64(1)	0.19
O(3)−C(3)	2.71(1)	−32.35(1)	0.19
O(4)−C(4)	2.75(1)	−35.02(1)	0.20
O(5)−H(5A)	2.64(8)	−39.6(5)	0.03
O(5)−H(5B)	2.36(7)	−23.3(4)	0.04
O(6)−H(6A)	2.62(9)	−41.2(5)	0.02
O(6)−H(6B)	2.35(7)	−36.0(5)	0.03
O(7)−H(7A)	2.65(8)	−32.7(4)	0.02
O(7)−H(7B)	2.40(7)	−33.5(4)	0.04
	(b) Croconate		
C(1)−C(2)	1.82(1)	−12.27(1)	0.22
C(2)−C(3)	1.82(1)	−12.31(1)	0.22
C(3)−C(4)	1.82(1)	−12.53(1)	0.18
C(4)−C(5)	1.80(1)	−11.78(3)	0.25
C(1)−C(5)	1.81(1)	−12.18(3)	0.22
O(1)−C(1)	2.67(1)	−28.35(2)	0.14
O(2)−C(2)	2.67(1)	−28.15(1)	0.15
O(3)−C(3)	2.66(1)	−27.68(1)	0.14
O(4)−C(4)	2.64(1)	−27.01(1)	0.14
O(5)−C(5)	2.68(2)	−28.49(10)	0.14
O(10)−H(10A)	2.70(9)	−25.5(6)	0.04
O(10)−H(10B)	2.90(9)	−23.2(5)	0.01
O(11)−H(11A)	2.55(10)	−32.1(6)	0.04
O(11)−H(11B)	2.77(9)	−29.5(7)	0.02
O(12)−H(12A)	2.93(9)	−26.4(6)	0.05
O(12)−H(12B)	2.92(9)	−42.2(7)	0.06

[a] ρ (eÅ^{-3}) is the electron density, $\nabla^2\rho$ (eÅ^{-5}) is the Laplacian, and ϵ is the ellipticity.

consideration.[32] The important bond parameters are the total density at the critical point (ρ_{BCP}) and its Laplacian, $\nabla^2\rho_{BCP}$, and ellipticity, ϵ. The value of ρ_{BCP} is a measure of bond strength, whereas the Laplacian signifies the extent of depletion or concentration of the bonding density. The ellipticity, which is related to the ratio of the curvatures along the minor and the major principal axes perpendicular to the bond, measures the extent of conjugation. The geometrical parameter, *d*, which is the perpendicular distance of the BCP from the internuclear axis, characterizes the strain in the bond. An estimate of bond polarization, Δ%, obtained from the location of the BCP with respect to the bonding atoms, is helpful in describing relative electronegativities of the atoms involved.

The critical point analysis in the bonding regions of the squarate and the croconate anions reveals (3, −1) CPs (Table 2). The ρ_{BCP} values for the C−C bonds of the squarate ion fall in a narrow range of 1.85(1)−1.87(1) e Å^{-3}. Those of the croconate ion are slightly lower with a mean value of 1.81(1) e Å^{-3}, but their spread is similar (∼0.01 e Å^{-3}). The Laplacians also behave in a likewise manner. The magnitude of the Laplacian are somewhat higher (∼−13.4(3) e Å^{-5}) in the squarate than in the croconate (∼−12.2(3) e Å^{-5}).[33] The ellipticity (ϵ) values in squarate vary between 0.23 and 0.27, with a mean value of 0.25 and those in croconate, are somewhat lower, between 0.18 and 0.25 with the mean value at 0.22 (Table 2). The mean *d* value for the C−C bonds in the squarate ring is 0.058 Å, whereas for the croconate the value is much smaller, 0.015 Å, in accordance with the observed strain in the rings (see Figure 3). The mean C−O bond density of the squarate ion is 2.72(3) e Å^{-3} as compared to 2.66(2) e Å^{-3} in the croconate ion. The pseudoatomic charges on the carbonyl oxygens are −0.15 e in the squarate and −0.13 e in the croconate ion. The charge on the squarate ring carbon is −0.14 e, and in the croconate, the carbon atom carries a smaller charge (−0.07 e). Accordingly, the C−O bond appears to be less polarized in squarate (Δ ∼ 18%) compared to croconate (Δ ∼ 25%).

The ρ_{BCP} values in the C−C regions of the rings in the two dianions are considerably lower compared to those encountered in a benzenoid ring. Thus, the naphthyl ring of 1,8-bis-(dimethylamino)naphthalene exhibits a C−C bonding density of ∼2.15 e Å^{-3}.[3b] The values of the squarate and the croconate rings are rather close to the density in a typical single bond (ρ_{BCP}, 1.71 e Å^{-3}). Following Cremer and Kraka,[32] the densities in the squarate and the croconate ions correspond to the bond order values of 1.19 and 1.12, respectively. These values may be contrasted with the bond orders of 1.62 in benzene[32] and 1.54 in the naphthyl ring of 1,8-bis(dimethylamino)naphthalene.[3b] This is probably because the π-acceptor carbonyl groups in the dianions withdraw the electron density away from the ring. The larger the number of carbonyl groups, the greater is the charge separation between the carbonyl oxygens and the carbocyclic ring and lower is the C−C bond order. The ellipticity values, however, actually compare well with the value for benzene (0.23).[31] The group charges associated with the squarate and the croconate ions are −1.16 and −1.04 e, respectively. However, a comparison of our results with those obtained from theory[22] is not straightforward because the latter is based on isolated dianions.

The densities and Laplacian values of the O−H···O bonds formed by the dianions with the water molecules indicate that these interactions are of moderate strength. In the squarate salt, for example, one of the three hydrogen bonds formed by the atom O(2) has a ρ_{BCP} value of 0.23(3) e Å^{-3} and a Laplacian of 4.4(3) e Å^{-5}. The other two O−H···O bonds carry smaller densities (∼0.11 e Å^{-3}) and Laplacians (∼3.0 e Å^{-5}) and therefore are much weaker. The ρ_{BCP} and the Laplacians of the O−H···O bonds formed by the oxygen atoms of the croconate ring are in the range 0.09−0.20 e Å^{-3} and 2.5−3.0 e Å^{-5}, respectively. Acceptors O(1) and O(5) that form linear hydrogen bonds have densities and Laplacians of the order of ∼0.10 e Å^{-3} and ∼2.0 e Å^{-5}, respectively. On the other hand, both O(2) and O(3) form bifurcated bonds that have ρ_{BCP} values in the range ∼0.10−0.20 e Å^{-3} and $\nabla^2\rho_{BCP}$ ∼ 2.0−3.0 e Å^{-5}. The small and positive Laplacians for all the hydrogen bonds formed by the squarate and the croconate anion rings show that they are closed-shell interactions.

We have analyzed the topological properties of the ring densities of the two systems. Figure 4 shows how ρ (normalized with respect to ρ_{BCP}) varies along a perpendicular line passing through the BCP of a C−C bond in the squarate and the croconate rings. Both the anion rings exhibit second-order saddles: (3, +1) at the ring centers. The densities associated with the ring critical points (RCPs) for the squarate and the croconate rings are 0.59(1) and 0.30(2) e Å^{-3}, respectively. As shown in Figure 4, the density variation outside the rings is similar irrespective of the ring size. This variation is extrapolated to inside the ring to represent the case of "an isolated bonding density". The variation of the charge density inside the ring, however, deviates significantly from the "isolated bond density" due to contributions from the other bonds forming the ring. The deviation is more significant in the case of the squarate than the croconate due to the smaller ring size. Accordingly, the density at the squarate RCP is higher. This finding goes well with Bader's argument on charge densities at RCPs.[31,34] Interestingly, the Laplacians at the RCPs, $\nabla^2\rho_{RCP}$ also show a

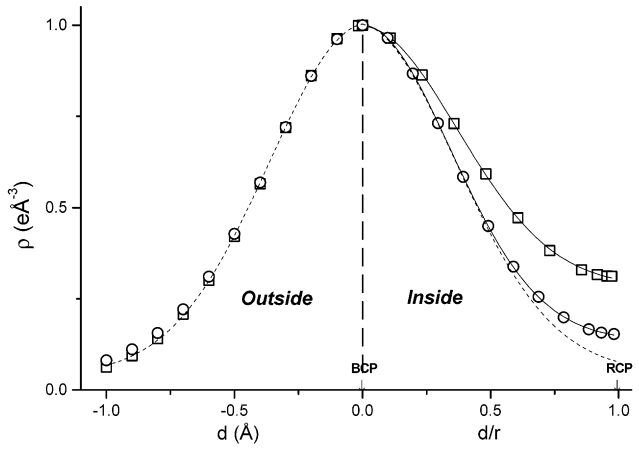

Figure 4. Total electron density profile in the squarate (squares) and the croconate (circles) rings along a line perpendicular to a C−C bond passing through its BCP. The density has been normalized with respect to the density at BCP. The distance from the BCP inside the ring region is normalized with respect to the distance, *r*, between BCP and RCP.

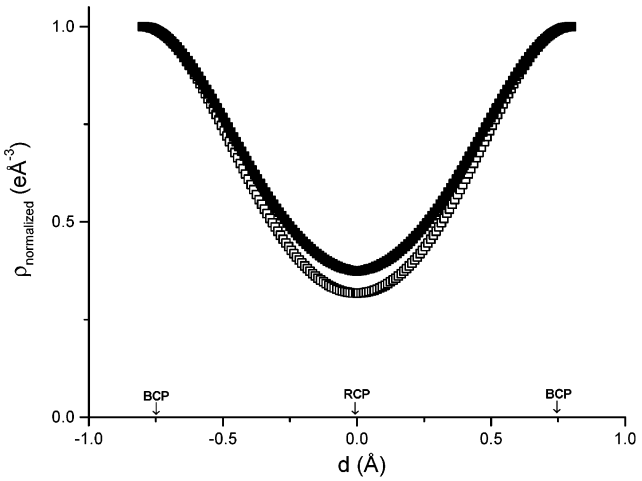

Figure 5. Total electron density profile in the squarate (open squares) and the cyclobutyl ring (solid squares) regions along a line joining two opposite BCPs (passing through the RCP). The density has been normalized with respect to the density at BCP.

similar trend. The squarate and the croconate rings exhibit $\nabla^2\rho_{RCP}$ values of 11.8(1) and 5.4(4) e Å^{-5}, respectively.

It is instructive to examine whether the charge density descriptors at RCP may be useful in describing aromaticity of the rings. For this purpose, we compiled the RCP parameters of several examples of cyclic systems from the literature, aromatic as well as nonaromatic, investigated either experimentally or theoretically. These include benzene,[35] substituted phenyl rings,[36−39] naphthyl rings,[3] uracil,[6] quinoid,[8] and phosphazene rings,[40] besides the rings formed by intramolecular hydrogen bonds.[36,41] Examples of smaller ring systems from the literature are pyrrolidine,[8] bis(thiodimethylene)tetrathiafulvalene rings,[42] the cyclobutyl ring of a truxillic acid,[38] and cyclopropyl rings.[35] We find that all the six-membered rings,[8,35−40] irrespective of whether they are aromatic or nonaromatic, exhibit ρ_{RCP} values in the range 0.10−0.19 e Å^{-3}. Similarly, the ρ_{RCP} values of the five-membered pyrrolidine and bis(thiodimethylene)tetrathiafulvalene rings fall in the range 0.24−0.36 e Å^{-3} whereas the four-membered squarate from this study and the cyclobutyl ring carry a density of ∼0.6 e Å^{-3}. We have also examined the Laplacian values of the ring systems under consideration. Comparing the squarate dianion and the cyclobutyl ring, we found the Laplacian values to be considerably different (11.8 and 5.8 e Å^{-5}, respectively), unlike the densities. It is rather surprising that the Laplacian values can be so different even though the two rings possess similar geometries. The origin of this difference can be understood in terms of the variation of ρ within the two rings. In Figure 5, we show the variation of ρ across their RCP regions. The rate of fall of density toward RCP is higher in the squarate compared to the cyclobutyl ring, the latter showing a somewhat flat profile at the RCP. Accordingly, its $\nabla^2\rho_{RCP}$ value, which is a measure of curvature, is lesser than that of the squarate ring. The higher Laplacian of the squarate anion is clearly an outcome of the high degree of conjugation prevalent in it. A similar effect, though to a lesser extent, is seen in the case of the croconate ion when compared with nonaromatic, five-membered rings. The Laplacian of the croconate ring is 5.4 e Å^{-5}, whereas the nonaromatic rings have $\nabla^2\rho_{RCP}$ values of approximately 4 e Å^{-5}.

An examination of the variation of the Laplacian with the ρ_{RCP} in ring systems yields useful insights. Thus, the plot presented in Figure 6 reveals the variation of $\nabla^2\rho_{RCP}$ to be markedly different for aromatic and nonaromatic systems. The aromatic systems seem to follow a trend where $\nabla^2\rho_{RCP}$ is

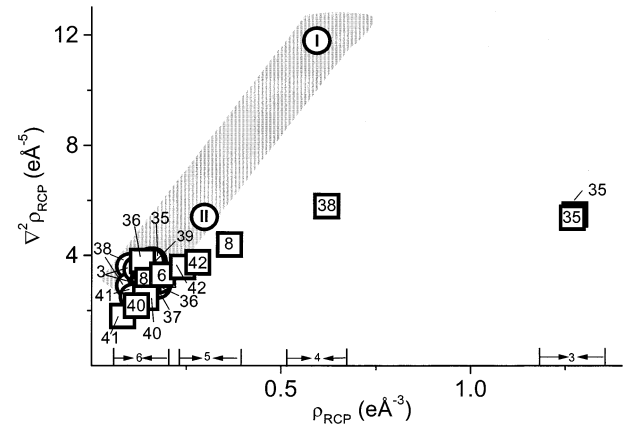

Figure 6. Plot of $\nabla^2\rho_{RCP}$ versus ρ_{RCP} for the *n*-membered cyclic systems (n = 3, 4, 5, 6). The circles depict aromatic rings, and the squares, the nonaromatic. The corresponding reference numbers are indicated inside the symbols. The data points denoted by **I** and **II** refer to the squarate and the croconate rings, respectively, from this study. The hashed region is where the Laplacian varies proportional to the density.

roughly proportional to ρ_{RCP} and, thus, fall into the hashed region in Figure 6. In nonaromatic systems, the $\nabla^2\rho_{RCP}$ values are much lower and do not exhibit any systematic trend. However, this distinction is not so clear in the case of the six-membered rings. The ρ_{RCP} and $\nabla^2\rho_{RCP}$ values of benzene are 0.16 e Å^{-3} and 3.81 e Å^{-5}, respectively, which indeed do not differ much from the values exhibited by the nonaromatic 5-nitrouracil ring (0.19 e Å^{-3}, 3.3 e Å^{-5}). The quinoid ring in 7,7-di(*S*(+)-2-(methoxymethyl)pyrrolidino)-8,8-dicyanoquinodimethane with its partial benzenoid character induced by the donor and acceptor groups, carries a ρ_{RCP} value of 0.15 e Å^{-3} and a Laplacian of 3.1 e Å^{-5}. Interestingly, the nonaromatic ring formed by a strong intramolecular hydrogen bond in benzoyl acetone[36] lies quite close to benzene in Figure 6. The substituted phenyl rings[36−39] cluster below the benzene point in Figure 6. The ρ_{RCP} and Laplacian values corresponding to the nonaromatic cyclophosphazenes[40] are much lower compared to benzene and substituted phenyl rings. The hydrogen-bonded seven-membered maleate ring[41] lies below phosphazenes with ρ_{RCP} and $\nabla^2\rho_{RCP}$ as low as 0.08 e Å^{-3} and 1.8 e Å^{-5}, respectively. The case of cyclopropane, however, deserves special mention. Besides carrying a relatively high density at RCP[35] (∼1.28 e Å^{-3}), the cyclopropyl ring exhibits bond ellipticities that are actually comparable to

those of double bonds, a property that accounts for its ability to act like a π system.[34] However, the nonaromatic nature of the cyclopropyl ring is clearly evident from Figure 6 where it falls considerably below the aromatic regime. Thus, the plot of $\nabla^2\rho_{RCP}$ versus ρ_{RCP} in Figure 6 appears to reflect the true aromatic character of cyclic systems.

Conclusions

An experimental charge density analysis of the squarate and croconate dianions has been carried out on the basis of low-temperature X-ray crystal data. The dianion rings are planar with all the C−C and C−O bond lengths in each ring being nearly equal. Charge density analysis reveals that all the C−C bond critical points in a ring carry equal densities and Laplacians, implying that the rings may be conjugated. The smaller squarate ring is more strained than the croconate, as evidenced by the outward bulging of the deformation density contours. The density and the Laplacian values at the ring critical point (RCP) of the squarate are much higher (0.6 e Å^{-3}, 11.8 e Å^{-5}) than those in the croconate (0.3 e Å^{-3}, 5.4 e Å^{-5}). A plot of the Laplacian versus density at RCP of the two systems along with a number of cyclic systems of different sizes gathered from the literature shows how one can distinguish aromatic and nonaromatic systems. The aromatic rings fall in a region where the Laplacian is roughly proportional to the density, and the nonaromatics show no definitive trend. The plot may be useful in the case of polycyclic systems where aromatic and nonaromatic rings coexist.

Supporting Information Available: Tables of bond distances, libration corrections, multipole populations, and spherical refinement data and contour plots. This material is available free of charge via the Internet at http://pubs.acs.org.

Acknowledgment. The authors thank Professor C.N.R. Rao F.R.S. for useful discussions and encouragement.

References and Notes

(1) Koritsanszky, T. S.; Coppens, P. *Chem. Rev.* **2001**, *101*, 1583.
(2) Kulkarni, G. U.; Gopalan, R. S.; Rao, C. N. R. *J. Mol. Struct.* (THEOCHEM) **2000**, *500*, 339.
(3) (a) Mallinson, P. R.; Wozniak, K.; Smith, G. T.; McCormack, K. L.; Yufit, D. S. *J. Am. Chem. Soc.* **1997**, *119*, 11502. (b) Mallinson, P. R.; Wozniak, K.; Wilson, C. C.; McCormack, K. L.; Yufit, D. S. *J. Am. Chem. Soc.* **1999**, *121*, 4640.
(4) (a) Koritsanszky, T.; Flaig, R.; Zobel, D.; Krane, H.-G.; Morgenroth, W.; Luger, P. *Science* **1998**, *279*, 356. (b) Dahaoui, S.; Pichon-Pesme, V.; Howard, J. A. K.; Lecomte, C. *J. Phys. Chem.* **1999**, *A103*, 6240.
(5) Fkyerat, A.; Guelzim, A.; Baert, F.; Zyss, J.; Perigaud, A. *Phys. Rev. B.* **1996**, *53*, 16236.
(6) Gopalan, R. S.; Kulkarni, G. U.; Rao, C. N. R. *Chem. Phys. Chem.* **2000**, *1*, 127.
(7) Madsen, G. K. H.; Krebs, F. C.; Lebech, B.; Larsen, F. K. *Chem. Eur. J.* **2000**, *6*, 1797.
(8) Gopalan, R. S.; Kulkarni, G. U.; Rao, C. N. R. *New J. Chem.* **2001**, *25*, 1108.
(9) Gomes, J. A. N. F.; Mallion, R. B. *Chem. Rev.* **2001**, *101*, 1349.
(10) Cameron, T. S.; Borecks, B.; Kwiatkowski, W. *J. Am. Chem. Soc.* **1994**, *116*, 1211.
(11) Spackman, M. A.; Goeta, A. E.; Howard, J. A. K.; Yufit, D. S. Private communication.
(12) Roversi, P.; Barzaghi, M.; Merati, F.; Destro, R. *Can. J. Chem.* **1996**, *74*, 1145.
(13) Destro, R.; Merati, F. *Acta Crystallogr.* **1995**, *B51*, 559.
(14) Stewart, R. F. In *Applications of Charge Density Research to Chemistry and Drug Design*; Jeffrey, G. A., Piniella, J. F., Eds.; Plenum: New York, 1991.
(15) Fuhrmann, P.; Koritsanszky, T.; Luger, P. *Z. Kristallogr.* **1997**, *212*, 213.
(16) Howard, S. T.; Krygowski, T. M. *Can. J. Chem.* **1997**, *75*, 1174.
(17) (a) West, R.; Niu, H.-Y.; Powell, D. L.; Evans, M. V. *J. Am. Chem. Soc.* **1960**, *82*, 6204. (b) West, R.; Niu, H.-Y. *J. Am. Chem. Soc.* **1962**, *81*, 1324.
(18) West, R.; Powell, D. L. *J. Am. Chem. Soc.* **1963**, *85*, 2577.
(19) Hess, B. A.; Jr.; Schaad, L. J.; Agranat, I. *J. Am. Chem. Soc.* **1978**, *100*, 5268.
(20) (a) Aihara, J. *J. Am. Chem. Soc.* **1976**, *98*, 2750. (b) Aihara, Junichi. *J. Am. Chem. Soc.* **1981**, *103*, 1633.
(21) (a) Serratosa, F. *Acc. Chem. Res.* **1983**, *16*, 170. (b) Jug, K. *J. Org. Chem.* **1983**, *48*, 1344. (c) Puebla, C.; Ha, T. K. *THEOCHEM* **1986**, *137*, 171.
(22) Schleyer, P v R.; Najafian, K.; Kiran, B.; Jiao, H. *J. Org. Chem.* **2000**, *65*, 426.
(23) Quiñonero, D.; Garau, C.; Frontera, A.; Ballester, P.; Costa, A.; Deya, P. M. *Chem. Eur. J.* **2002**, *8*, 433.
(24) Allen, F. H.; Kennard, O.; Watson, D. G.; Brammer, L.; Orpen, A. G.; Taylor, R. *J. Chem. Soc., Perkin Trans. II* **1987**, S1.
(25) Koritsanszky, T.; Howard, S. T.; Richter, T.; Mallinson, P. R.; Su, Z.; Hansen, N. K. *XD, A computer program package for multipole refinement and analysis of charge densities from diffraction data*. Cardiff, Glasgow, Buffalo, Nancy, Berlin, 1995.
(26) A second refinement has been carried out in which the sodium ion is treated as spherical (core-only scattering) and the chemical equivalence constraint on the ring oxygen atoms removed (supplementary Tables 4 and 5). In the literature, we find both types of refinements adopted for the sodium ions. For example, Ichikawa et al. (Ichikawa, M.; Gustafsson, T.; Olovsson, I. *Acta Crystallogr.* **1998**, *B54*, 29) employed hexadecapole refinement, whereas Bak et al. (Bak, H. P.; Olovsson, I.; McIntyre, G. J. *Acta Crystallogr.* **1998**, *B54*, 600) imposed spherical symmetry on sodium ions.
(27) Hirshfeld, F. L. *Acta Crystallogr.* **1976**, *A32*, 239.
(28) Busetti, V.; Marcuzzi, F. *Z. Kristallogr.* **1997**, *212(4)*, 302.
(29) Dunitz, J. D.; Seiler, P.; Czechtizky, W. *Angew. Chem., Int. Ed. Engl.* **2001**, *40*, 1779.
(30) Lee, C-R.; Wang, C-C.; Chin, K-C.; Lee, G-H.; Wang, Yu. *J. Phys. Chem. A* **1999**, *103*, 156.
(31) Bader, R. F. W. *Atoms in Molecules—A quantum theory*; Clanderon Press: Oxford, U.K., 1990.
(32) Cremer, D.; Kraka, E. *Croat. Chem. Acta* **1984**, *57*, 1259.
(33) The results obtained from the second refinement procedure (treating sodium ions as spherical and removing constraints on the ring oxygen atoms) differ only slightly from those of the original refinement. The ρ_{BCP} values of the C−C bonds in the squarate ring fall in the range of 1.84−1.86 e Å^{-3}, whereas for croconate, it is ∼1.82 e Å^{-3}. The Laplacians exhibit a similar spread as in the original refinement (see supplementary Table 5). Ring critical point descriptors also do not differ significantly.
(34) Bader, R. F. W.; Slee, T. S.; Cremer, D.; Kraka, E. *J. Am. Chem. Soc.* **1983**, *105*, 5061.
(35) Zhang, Y− H.; Hao, J- K.; Wang, X.; Zhou, W.; and Tang, T- H. *J. Mol. Struct. (THEOCHEM)* **1998**, *455*, 85.
(36) Madsen, G. K. H.; Iversen, B. B.; Larsen, F. K.; Kapon, M.; Reisner, G. M.; Herbstein, F. H. *J. Am. Chem. Soc.* **1998**, *120*, 10040.
(37) Gopalan, R. S.; Kulkarni, G. U.; Subramanian, E.; Renganayaki, S. *J. Mol. Struct.* **2000**, *524*, 169.
(38) Gopalan, R. S.; Kulkarni, G. U. *Proc. Ind. Acad. Sci.* **2001**, *113*, 307.
(39) Bach, A.; Lentz, D.; Luger, P. *J. Phys. Chem. A* **2001**, *105*, 7405.
(40) Luana, V.; Pendas, A. M.; Costales, A.; Carriedo, G. A.; Garcia-Alonso, F. J. *J. Phys. Chem. A* **2001**, *105*, 5280.
(41) Madsen, D.; Flensburg, C.; Larsen, S. *J. Phys. Chem. A* **1998**, *102*, 2177.
(42) Espinosa, E.; Molins, E.; Lecomte, C. *Phys. Rev. B* **1997**, *56*, 1820.